



GLOBAL JOURNAL OF RESEARCHES IN ENGINEERING: E
CIVIL AND STRUCTURAL ENGINEERING
Volume 19 Issue 1 Version 1.0 Year 2019
Type: Double Blind Peer Reviewed International Research Journal
Publisher: Global Journals Inc. (USA)
Online ISSN: 2249-4596 & Print ISSN: 0975-5861

Nonlinear Analysis of Edge Joint on T-Shaped Concrete-Filled Steel Tubular Column-H-Shaped Steel Beam Seismic Performance based on ABAQUS

By Yadong Bian, Yichuan Tian, Yi Zhao, Long Cheng, Cheng Hong, Zhicheng
Zhicheng Gao & Jiliang Li

Beihang University

Abstract- To comprehensively analyze the seismic performance and failure modes of edge joint, which is composed of T-shaped concrete-filled steel tubular column and H-shaped steel beam, the joint was imposed through low frequency cycling loading. Model of edge joint was established by the nonlinear finite element software ABAQUS. The effect of different parameters, such as axial compression ratio and side plate extension length, on the seismic performance were simulated. The results indicates that the buckling of the steel beam occurs at the lateral extension of the side plate due to the strengthening of the side plate; the axial compression ratio has no obvious effect on the ultimate load; the increase of the side plate length can effectively improve the ultimate load.

Keywords: t-shaped concrete-filled steel tubular column; H-shaped steel beam; Seismic performance of joint; finite element analysis.

GJRE-E Classification: FOR Code: 090599



Strictly as per the compliance and regulations of:



© 2019. Yadong Bian, Yichuan Tian, Yi Zhao, Long Cheng, Cheng Hong, Zhicheng Gao & Jiliang Li. This is a research/review paper, distributed under the terms of the Creative Commons Attribution-Noncommercial 3.0 Unported License (<http://creativecommons.org/licenses/by-nc/3.0/>), permitting all non commercial use, distribution, and reproduction in any medium, provided the original work is properly cited.

Nonlinear Analysis of Edge Joint on T-Shaped Concrete-Filled Steel Tubular Column-H-Shaped Steel Beam Seismic Performance based on ABAQUS

Yadong Bian ^α, Yichuan Tian ^σ, Yi Zhao ^ρ, Long Cheng ^ω, Cheng Hong [¥], Zhicheng Gao [§] & Jiliang Li ^χ

Abstract- To comprehensively analyze the seismic performance and failure modes of edge joint, which is composed of T-shaped concrete-filled steel tubular column and H-shaped steel beam, the joint was imposed through low frequency cycling loading. Model of edge joint was established by the nonlinear finite element software ABAQUS. The effect of different parameters, such as axial compression ratio and side plate extension length, on the seismic performance were simulated. The results indicates that the buckling of the steel beam occurs at the lateral extension of the side plate due to the strengthening of the side plate; the axial compression ratio has no obvious effect on the ultimate load; the increase of the side plate length can effectively improve the ultimate load.

Keywords: *t-shaped concrete-filled steel tubular column; H-shaped steel beam; seismic performance of joint; finite element analysis.*

1. INTRODUCTION

The frame structure of concrete-filled steel tubular special-shaped columns and steel beams has attracted increasing applications in high-rise buildings and long span bridges. It not only has high bearing capacity of concrete-filled steel tube (CFST), good deformation capacity and overcomes the disadvantage of special shaped reinforced concrete structure, but also steel tube can be served as form work to pure core concrete, and saves the constructing cost of using formwork, and accelerates the constructing speed [1]. The frame structure composed of concrete-filled steel tubular columns and steel beam has become a kind of seismic structure with many applications. At present, the joints mainly adopt outer-diaphragm, internal-diaphragm, bearing pin and so on rigid connection or hinge connection form [2]. According to the distribution position of the frame column, the composite joints can be divided into the

edge joint, the angular joint and the middle joint. The edge joint is connected by the edge column of frame structure and the beam. The thickness of flange on T shape column is equal to the thickness of wall. No matter CFST or Reinforced Concrete (RC) is the same, the seismic performance is different. However, the joint is the key part of the composite structure design, its rationality is directly related to the safety of the structure and the economy of the project. Many different joint sizes, joint categories and connection types have been used in various engineering for different requirements. Thus, in order to obtain the seismic behaviors of the composite joint, it is necessary to study the influence, with the change of axial compression ratio and side plate extension length.

In recent years, many scholars have studied the seismic behaviors of different kinds of composite joints on various structure by analytical, experimental and finite element (FE) simulation methods. While, most of them focus on other types of steel tubular special-shaped column-steel beam frame joints. The seismic behavior of joint on T-shaped CFST and H-shaped steel beam is less studied. The domestic scholars have put forward a variety of joint forms on CFST columns and carried out experimental research and theoretical analysis [3-9]. Zhou Peng et al. [1] studied the failure characteristics and seismic performance of rectangular steel tubular special-shaped column-steel beam frame joints. Foreign scholars such as Ataei et al. [10] studied the end-plate connection joint in the beam-column composite joint. Hwang et al. [11] studied the seismic behavior of the joint of U-shaped steel-concrete composite beams and RC columns. XU et al. [12] analyzed the seismic behavior of cross section joints of CFST columns and steel girders under different axial compression ratios. Fukumoto et al. [13] studied the joint specimens of high-strength steel tubular columns and steel beam, and the types of the joints include inner partition joint of square steel tubular columns-steel beam and outer partition joint of concrete circular steel tube-steel beam. Kubota et al. [14] proposed a separate type of outer diaphragm joint with square Steel tubular column and H-shaped steel beam, which is less welding work and easier to

*Author α ρ ω ¥: School of Civil Engineering and Architecture, Zhongyuan University of Technology, China.
e-mail: zg8@zips.uakron.edu*

Author σ: School of Transportation Science and Engineering, Beihang University, China.

Author §: Department of Civil Engineering, University of Akron, USA.

Author χ: Department of Mechanical and Civil Engineering, Purdue University Northwest, USA.

construct than the traditional outer-diaphragm. The experimental results show that the mechanical properties of the separated outer-diaphragm joint is similar to the traditional outer diaphragm. Peng Zhong et al. [15] proposed experimental and numerical studies on the seismic performance of the new end-plate connection between T-shaped CFST columns and reinforced concrete (RC) beams with slabs. Peng Zhong et al. [16] studied seismic behaviour of innovative ringbar reinforced connections composed of T-shaped CFST columns and RC beams with slabs. The comparison between the FE analysis and the experimental results demonstrates the accuracy of the proposed model. Hosseini Farshid et al. [17] investigated the use of engineered cementitious composites (ECC) in 3-D exterior beam-column connections to improve building seismic performance. Mou Ben et al. [18] done an experimental investigation on the seismic behavior of a novel steel concrete composite beam-to-column connections reinforced by outer-annular-stiffener.

In this paper, the joint form of T shaped CFST columns-H steel beam is proposed. The failure mode and seismic performance of T-shaped CFST column-H-shaped steel beam joint is studied, based on the nonlinear finite element software ABAQUS.

II. ESTABLISHMENT OF FINITE ELEMENT MODEL

T-shaped CFST column-H-shaped steel beam edge joint is welded by T-shaped CFST column and H-shaped steel beam, and is reinforced by side panels. Fig.1 shows the specimen size and large sample. The T-shaped CFST column section size, wall thickness of steel tube, column height and steel beam size are 300mm×100mm×200mm×100mm, 5mm, 1800mm, and 250mm×100mm×4mm×4mm, respectively. The properties of steel material are presented in Table 1. The mechanical properties of concrete are shown in Table 2. The finite element model number and parameters settings are summarized in Table 3.

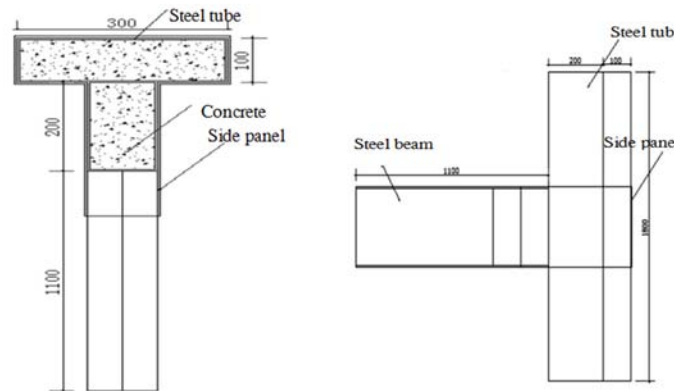


Fig. 1: Joint large sample

Table 1: Material properties of steel

Steel model	Elastic modulus	Yield strength	Ultimate strength	Poisson's ratio
Q235	$2.06 \times 10^5 \text{Mpa}$	235Mpa	370Mpa	0.3

Table 2: Mechanical properties of concrete

Concrete strength grade	Elastic modulus	Axial compressive strength standard value	Axial compressive strength design value	Poisson's ratio
C40	$3.25 \times 10^4 \text{Mpa}$	26.8Mpa	19.1Mpa	0.2

Table 3: Comparison of finite element model parameters

Model number	Axial compression ratio	Side plate extension length(mm)	Concrete strength grade	Steel model	Steel beam size(mm)
A	0.2	258	C40	Q235	250×100×4×4
B	0.4	258	C40	Q235	250×100×4×4
C	0.6	258	C40	Q235	250×100×4×4
D	0.6	308	C40	235	250×100×4×4
E	0.6	356	C40	Q235	250×100×4×4

The three-dimensional solid element (C3D8R) with eight-node reduced integral scheme is used to build the above-mentioned joint model, applying nonlinear finite element software ABAQUS. The model mainly includes T-shaped CFST columns, H-shaped steel beams and side plates. The properties of the finite element model are divided into two categories. First, the establishment of concrete properties, including elasticity and concrete damage plasticity, applied to the core concrete. Second, the establishment of steel properties, including elasticity and plasticity, applied to T-shaped steel tube, H-shaped steel beams and side panels. The interaction between the T-shaped steel tube, the H-shaped steel beam and the side plate is the "Tie" provided in ABAQUS. The interaction between the T-shaped steel tube and the core concrete, between the side plate and the core concrete, selects the "Surface-to surface contact" provided in ABAQUS, where the "Surface-to-surface contact" interaction between the T-shaped steel tube and the core concrete includes "Normal Behavior" and "Tangential Behavior", and the "Surface-to-surface contact" interaction between the side plate and the core concrete only includes "Normal Behavior".

The settings of the finite element models are depended on two loading steps. In the first step, the

side plate of the column top is coupled to the reference point XRP-2 and an axial concentrating force is applied at the reference point XRP-2. The axial pressure is designed to be 1882.78kN, and the vertical load of the column is loaded at the axial compression ratio of 0.2, 0.4 and 0.6, respectively. Afterwards, the beam end section is coupled with the reference point XRP-3, and apply a vertical periodic displacement on the reference point XRP-3. In the finite element model, all degrees of freedom in the bottom hinge are restrained. The displacement of the node in the horizontal direction is restricted at the loading end of the column, and the displacement of the node X direction is restricted at loading end of the beam, shown as Fig.2.

The meshing size has a great influence on the accuracy and computational efficiency of the finite element analysis software ABAQUS. If the size of the finite element model grid is too large, the calculating result of the finite element model may be deviate and even erroneous. If grid is too small, it will take long time to calculate the result. In order to ensure the accuracy of calculation and save the computational resources, the mesh size of the nodal domain is smaller than that of other parts in the process of finite element meshing. The grid diagram is shown as Fig. 3.

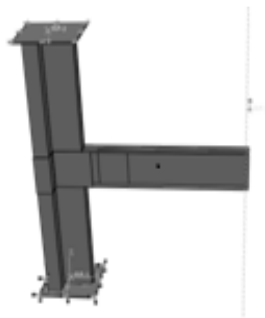


Fig. 2: Finite element model Fig.

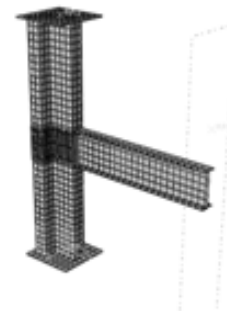


Fig. 3: Finite element meshing

III. FINITE ELEMENT CALCULATING RESULTS

a) Stress nephogram analysis

Fig. 4 shows the Mises stress distribution of four locations, including the T-shaped steel tube, the core concrete, the H-shaped steel beam and the side plate. From the figure, the stress of the steel tube is relatively larger on the upper and lower sides of the middle plate of the steel tube, and the stress of the nodal domain becomes smaller, and buckling of the T-shaped column occurs on the upside of side plate and the underside of the side plate. This is because the side plane assumes a lot of stress, to achieve a very good control. In the

corner of the core concrete, the stress is relatively larger, because the constraint of the square steel tube is weak in the corner of the core concrete; the stress at the upper and lower flanges of the steel beam joint domain is larger. Since the reinforcing plate constraints, buckling of steel beams occurs in the side plate portion epitaxial portion; the stress of the side plate is large, it plays a very good restraint to the core area of the steel tube, thus reducing the stress of the steel tube in the core area.

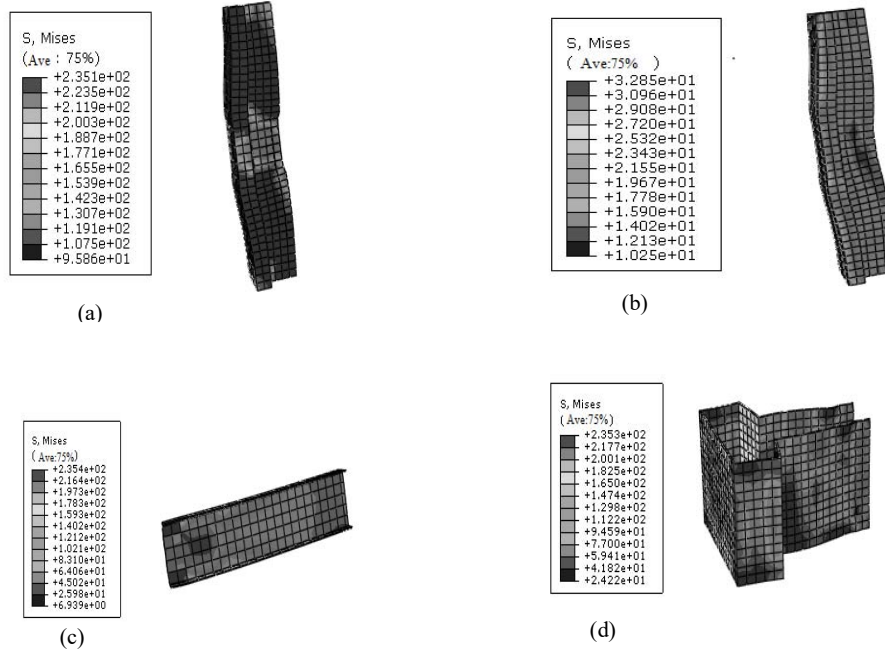
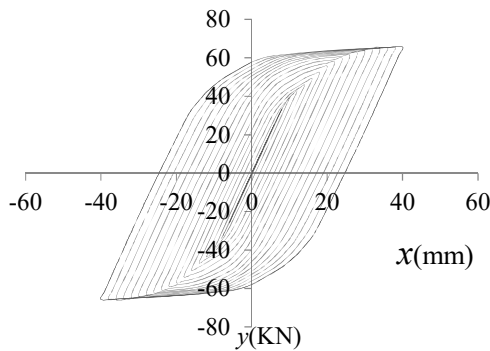


Fig. 4: Stress nephogram

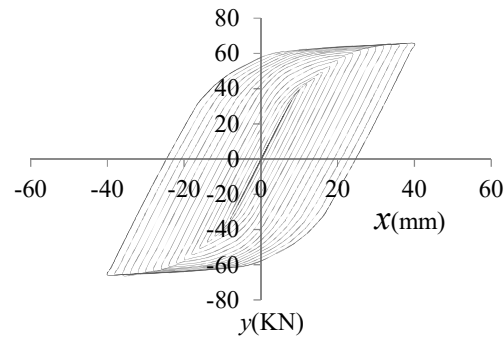
b) Load displacement curve

Fig. 5 is the hysteresis curve of each finite element model under the action of low frequency cycling loading. As shown in the figure 5, the hysteresis curves of the different axial compression ratios are universally similar. Before the yield, the curve reflecting the relationship between displacement and load is linear. The specimen is in the elastic stage. With the increase of the displacement load, the steel beam gradually

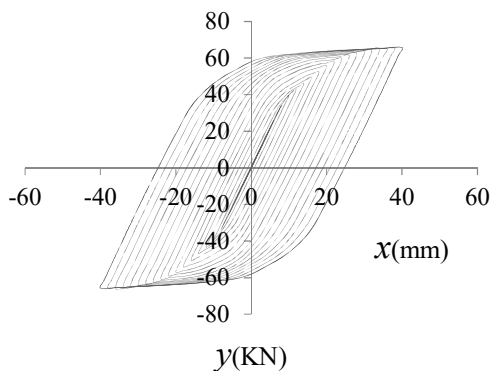
enters the plastic working stage. As the stiffness of the column is much larger than the stiffness of the beam, and the low frequency cycling loading is applied to the end of beam. The increase of the axial load ratio has no obvious effect on the ultimate load. The increase of the lateral extension of the side plate can effectively improve the ultimate load. The hysteresis curves of per models do not shrink, which are full of spindle, and showing good seismic performance of the composite joint.



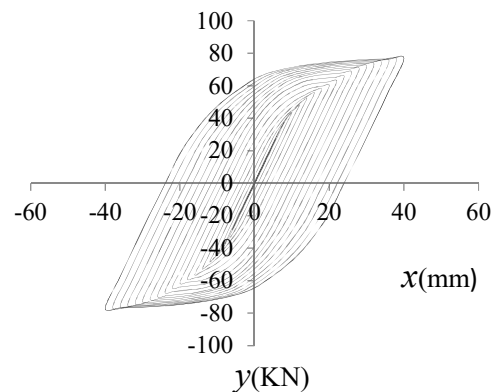
(a) C40, n=0.2, d=258mm



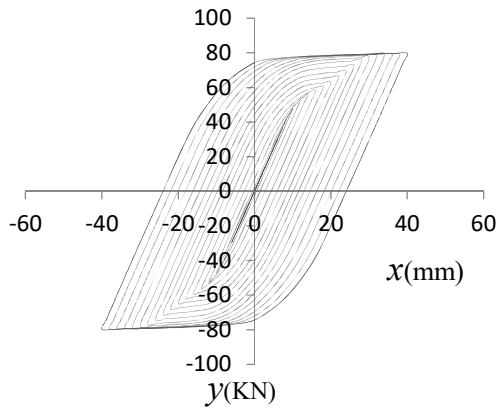
(b) C40, n=0.4, d=258mm



(c) C40, n=0.6, d=258mm



(d) C40, n=0.6, d=308mm



(e) C40, $n=0.6$, $d=358\text{mm}$
 Fig. 5: hysteresis curve

c) Node skeleton curve

Fig. 6 is a comparison of the skeleton curves obtained from the model hysteresis curves of Fig. 5. Fig. 6 (a) is a comparison chart of the skeleton curves corresponding to different axial compression ratios, and Fig. 6 (b) shows the skeleton curve comparison chart of different lateral extension length of the side plate. It can be seen from the figure that the axial compression ratio is similar to the corresponding skeleton curve. The increase of the axial compression ratio has no obvious effect on the ultimate load. The increase of the side plate length can effectively increase the ultimate load. When the lateral extension of the side plate is increased to a certain value, the effect of the increase of the side plate length on the ultimate load is reduced.

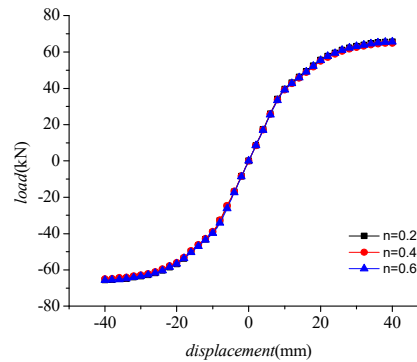
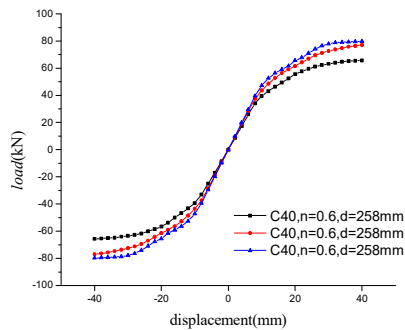


Fig. 6: Comparison of skeleton curves

d) Energy dissipation capacity

The deformation process of structural members under the action of low frequency cycling loading is also the process of absorbing energy. The energy dissipation capacity of structural members determines the seismic capacity of the structure. The energy dissipation capacity of the joint model is mainly evaluated by the equivalent viscous damping coefficient [19]. Usually, the average of the reinforced concrete joint is 0.1, and the common steel concrete joint is about 0.3 [20]. Table 4

shows the equivalent viscous damping coefficient corresponding to the hysteresis curve of each finite element model. As shown in the table 4, the equivalent viscous damping coefficient corresponding to each hysteresis curve is close to 0.2, it is larger than the equivalent viscous damping coefficient of the reinforced concrete beam which is 0.1. It indicates that the T shaped CFST column-H-shaped steel beam has good energy dissipation capacity and seismic capacity.

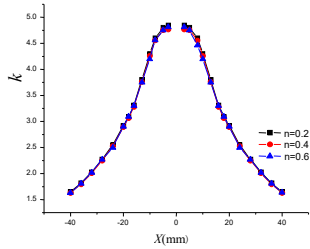
Table 4: The Equivalent viscous damping coefficient of each specimen

Model number	A	B	C	D	E
h_e	0.193	0.194	0.211	0.254	0.261

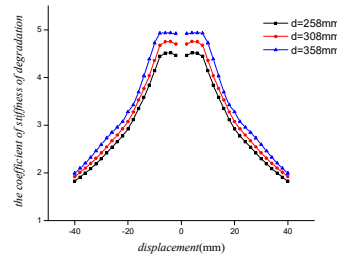
e) Stiffness degradation curve

Fig.7 is stiffness degradation curve comparison chart. Fig.7 (a) shows the stiffness degradation curves of the hysteresis curves for finite element models A, B, and C. Fig.7 (b) shows the stiffness degradation curves of the hysteresis curves for finite element models C, D, and E. It can be concluded from the graph that the variation law of the degenerate coefficient of the beam stiffness is normal distribution. With the increase of the beam displacement load, the stiffness degradation of

each model is obvious; the influence of the axial compression ratio on the degradation coefficient of the joint stiffness is not obvious. With the increase of the displacement of the side plate, the stiffness of the finite element model increases at the initial loading stage. As the displacement load increases, the loaded steel beam begins to enter the plastic work, and the difference of the stiffness of each member is smaller.



(a) Different axial compression ratio stiffness degradation curve



(b) Degradation curves of elongation stiffness of different side plates

Fig. 7: Stiffness degradation curve

IV. CONCLUSION

In this paper, the seismic performance of the joint is evaluated, based on the establishment of rationalized T-shaped CFST column-H-shaped steel beam edge joint finite element model. The conclusions are summarized as follows:

1. The buckling of the T column occurs on the upper and lower sides of the side plate, and the buckling of the steel beam occurs at the side plate extension, due to the restraint of the side plate.
2. The increase of the axial load ratio has no obvious effect on the ultimate load, and the increase of the length of the side plate can effectively improve the ultimate load of the beam end, as the stiffness of the column is much larger than the stiffness of the beam, and the low cyclic loading is applied to the beam end.
3. The equivalent viscous damping coefficient corresponding to each hysteresis curve is close to 0.2, which indicates that the T-shaped concrete-filled steel tubular column-H-shaped steel beam node has good energy dissipation capacity.

This paper studies the failure mode and seismic performance of T-shaped concrete-filled steel tubular columns-H-shaped steel beam node, application the finite element numerical simulation. In the future research, it is also necessary to combine finite element simulation with experimental research, and make a more thorough analysis of the node.

ACKNOWLEDGEMENTS

The authors would like to thanks the National Natural Science Foundation of China, Henan Province Science and Technology Research Project and Henan Province Higher Education Key Research Project Basic Research Project for financial support.

REFERENCES RÉFÉRENCES REFERENCIAS

1. Peng Zhou, Jianyang Xue, Xi Chen, et al. Experimental study on seismic performance of joints

between concrete-filled square steel tubular special-shaped columns and steel beams[J]. Journal of Building Structures, 2012, 33(8): 41—50. (in Chinese).

2. Han Linhai, Yang Youfu. Technology of modern concrete-filled steel tubular structures [M].China Architecture & Building Press, 2004(in Chinese).
3. Zhu Lei, Ye Jinsong. Finite element analysis of concrete behavior of concrete-filled square steel tubular joints [J]. Building Structures, 2011,S1: 1105-1108.
4. LUO Qin. Study on nonlinear finite element method of concrete-filled square steel tubular column and steel beam connection [J]. Journal of Three Gorges University (Natural Science Edition), 2010, 05: 45-47.
5. Ding Yongjun, Shang Kuijie, Wan Fanggui, Qin Ying. Experimental study and finite element analysis of seismic behavior of rectangular concrete-filled steel tubular column-H steel beam [J]. Journal of Building Structures, 2012, 02: 93-99.
6. Zhang Jicheng, Shen Zuyan, Lin Zhenyu, Luo Jinhui. Study on seismic behavior of L-shaped concrete-filled steel tubular frame structures [J]. Journal of Building Structures, 2010, 08: 1-7.
7. Xu Cheng xiang, Wan Bo, Zhang Ji cheng, Ma Jinjun. Study on seismic behavior of joints in concrete frame of cross-shaped concrete-filled steel tubular columns [J]. Building Structures, 2012, 03: 80-83.
8. Xu Cheng xiang, Wu Zanjun, Zeng Lei, Zhang Jicheng, Ma Jinjun. T- shaped concrete-filled steel tubular column - I-beam girder framework of the top edge of the seismic performance test [J].Journal of Building Structures, 2012, 08: 58-65.
9. Lin Mingsen, Dai Shaobin, Liu Jixiong, Peng Zhong. Experimental Study on Seismic Behavior of T-shaped Concrete Filled Steel Tubular Columns and Steel Beams [J].Journal of Seismic Engineering and Engineering Vibration, 2012, 02: 114-119.
10. ATAEI A, BRADFORD M A, LIU X P. Experimental study of flush end plate beam-to-column composite joints with precast slabs and deconstruct able

- bolted shear connectors[J]. Structures, 2016, 7 (1): 43-58.
11. HWANG H J, EOM T S, PARK H G, et al. Cyclic loading test for beam-column connections of concrete filled U-shaped steel beams and concrete-encased steel angle columns[J].Journal of Structural Engineering, 2015, 141 (:04015020.
 12. XU Y, ZHANG Y. Nonlinear finite element analysis on seismic behavior of joints of crisscross section column composed of core concrete-filled steel tube and steel beam in different axial compression ratio[J].International forum on energy, environment and sustainable development,2016, 75 (46) :68-74.
 13. Fukumoto T, Morita K. Elastoplastic behavior of panelzone in steel beam-to-concrete filled steel tube column moment connections[J].Journal of Structural Engineering, 2005, 131 (7) :1841-1853.
 14. Kubota Jun, Taki Masaya, Tsukamoto Kiyoshi, et al. Elasto-plastic behavior of connection between concrete-filledsquare steel tubular column and steel beam using splitexternal diaphragm[R].Annual Report, Kajima Technical Research Institute, Kajima Corporation,2007:65-70.
 15. Peng Z, Dai S, Pi Y, et al. Seismic performance of end-plate connections between T-shaped CFST columns and RC beams[J]. Journal of Constructional Steel Research, 2018, 145:167-183.
 16. Peng Z, Dai S, Pi Y, et al. Seismic behaviour of innovative ring-bar reinforced connections composed of T-shaped CFST columns and RC beams with slabs [J]. Thin-Walled Structures, 2018, 127: 1-16.
 17. Hosseini F, Gencturk B, Aryan H, et al. Seismic behavior of 3-D ECC beam-column connections subjected to bidirectional bending and torsion [J].Engineering Structures, 2018, 172: 751-763.
 18. Mou B, BaiY. Experimental investigation on shear behavior of steel beam-to-CFST column connections with irregular panel zone[J]. Engineering Structures, 2018, 168: 487-504.
 19. XU Y F, ZHU S J, XU P Y, et al. Seismic performance study on the joint of crisscross concretefilled steel tube column-steel beam in different axial compression ratios[J].Applied mechanics and materials, 2014, 578/579:252-255.
 20. XU Y F, ZHAI Z L, XU P Y. Analysis of seismic performance of the joint of cellular steel column and steel beam in different axial compression ratio[J].Applied mechanics and materials, 2014, 578/579:244-247.